ACS OMEGA

Open Access

http://pubs.acs.org/journal/acsodf

Article

Soil Biodegradation Resistance of Cotton Fiber Doped with Interior and Exterior Silver Nanoparticles

Sunghyun Nam,* Haile Tewolde, Zhongqi He, Kanniah Rajasekaran, Jeffrey W. Cary, Gregory Thyssen, Hailin Zhang, Christine Sickler, and Md Muhaiminul Islam

Cite This: *ACS Omega* 2024, 9, 13017−13027

Read Online

ACCESS | Metrics & More | Article Recommendations

ABSTRACT: Engineering fibers with nanomaterials is an effective way to modify their properties and responses to external stimuli. In this study, we doped cotton fibers with silver nanoparticles, both on the surface (126 ± 17 nm) and throughout the fiber cross section (18 ± 4 nm), and examined the resistance to soil biodegradation. A reagent-free one-pot treatment of a raw cotton fabric, where noncellulosic constituents of the raw cotton fiber and starch sizing served as reducing agents, produced silver nanoparticles with a total concentration of 11 g/kg. In a soil burial study spanning 16 weeks, untreated cotton underwent a sequential degradation process—fibrillation, fractionation, and merging—corresponding to the length of the soil burial period, whereas treated cotton did not exhibit significant degradation. The remarkable biodegradation resistance of the treated cotton was attributed to the antimicrobial properties of silver nanoparticles, as demonstrated through a test involving the soil-borne fungus *Aspergillus flavus*. The nonlinear loss behavior of silver from the treated cotton suggests that nanoparticle depletion in the soil depends on their location, with interior nanoparticles proving durable against environmental exposure.

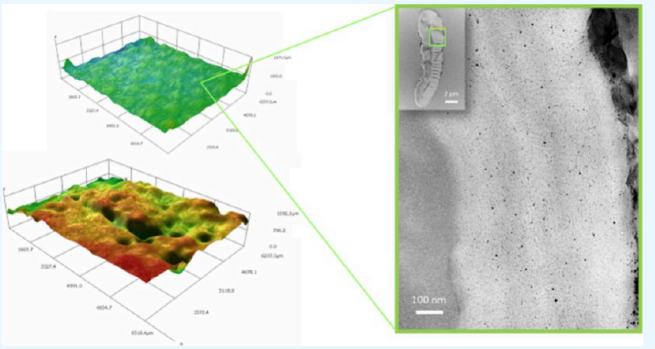

1. INTRODUCTION

Due to its great potential in enhancing properties, processes, and applications,[1−3] nanotechnology has found widespread adoption in the textile industry. Nanoparticle treatments empower textiles with various functionalities, including antimicrobial activity,[4−6] thermal properties,[7] electrical conductivity,[8,9] and optical properties.[10,11] However, fully harnessing nanotechnology's potential in textiles faces challenges. One key factor is that textile products, unlike many other consumer products, undergo routine washing or laundering. Most nanofinishing techniques for textiles have focused on surface-based treatments, involving processes like padding onto textiles,[12] or the synthesis of silver nanoparticles onto fabric surfaces.[13−15] Unfortunately, nanoparticles applied to the surface of textiles are susceptible to contamination and detachment caused by mechanical and chemical forces during the washing process, thus making them vulnerable to microbial contamination. For instance, silver nanoparticles, commonly used in producing odor-resistant or antimicrobial textiles, experience a substantial 25% loss after a single machine laundering[16,17] and over 80% loss after just five laundering cycles.[12] This lack of durability of nanoparticles not only compromises the performance of finished textiles but also poses potential health and environmental risks.

To enhance the binding capacity of nanoparticles to textiles, we have explored synthetic methods that enable the production of nanoparticles within cotton fibers.[18−26] One of these methods involves a natural synthetic method that leverages the noncellulosic components present in raw cotton fibers, including pectin, sugars, fatty alcohols, hemicellulose, and condensed tannins, as reducing agents.[22,25,26] This *in situ* synthesis technique results in the formation of nanocomposite substructures within cotton fibers without the need for external agents, such as reducing and stabilizing agents or chemical modifications of the cotton fibers. Remarkably, the nanoparticles embedded within the fibers exhibit persistent resistance to leaching, even after undergoing multiple laundering cycles. Since these nanoarchitectured cotton fibers are novel, there have been no previous studies investigating how the incorporation of silver nanoparticles influences the biodegradability of cotton fibers.

Received: November 24, 2023
Revised: January 31, 2024
Accepted: February 26, 2024
Published: March 6, 2024

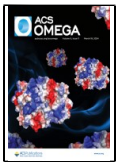

Here, we doped cotton fibers with silver nanoparticles, both on the surface and throughout the fiber cross-section, and conducted soil burial and antifungal studies. This distinctive nanostructured cotton fiber was obtained through a straightforward one-pot process involving raw cotton fabric sized with starch without the need for additional reducing or stabilizing agents. The presence of exterior and interior nanoparticles was confirmed by examining fiber cross sections using electron microscopy. We examined how the incorporated nanoparticles influenced the biodegradability and antifungal properties of the cotton fabrics in comparison to those of untreated control cotton fabrics and identified the depletion behavior of silver from the cotton fabric in the soil.

2. EXPERIMENTAL SECTION

2.1. Materials. Raw cotton plain woven fabric (graige cotton duck, 237 g/m^2) was purchased from Testfabrics Inc. (West Pittston, PA). Silver nitrate ($AgNO_3$) was purchased from J.T. Baker. Triton X-100, nitric acid (HNO_3), methyl methacrylate, butyl methacrylate, and benzoyl peroxide were purchased from Sigma−Aldrich. The cotton fabric and all chemicals were used as received. Deionized (DI) water was used as a solvent.

2.2. Preparation of Silver Nanoparticle-Doped Cotton. Rectangular samples (5 × 5 cm) were cut from the cotton fabric. In a 300 mL round-bottom flask, a 25 mL aqueous solution containing $AgNO_3$ (25 mM) and Triton X-100 (0.05 wt %) was prepared. Subsequently, a rectangular sample (approximately 2 g) was immersed in this prepared solution at room temperature overnight. With the setup of a condenser, the sample in the flask was heated to 100 °C and maintained at this temperature for 1 h. Following the heat treatment, the sample was washed in DI water multiple times and air-dried.

2.3. Soil Burial. The burial study was conducted in an agronomic field in a Leeper silty clay loam soil located at the R.R. Foil Plant Science Research Center of Mississippi State University, Mississippi State, MS from October 20, 2022 to February 9, 2023. The plot for the study was prepared by removing grass and any other vegetation on the surface with a mechanical scraper. The soil was then loosened using a backhoe to a depth of about 20 to 25 cm, and the surface was raked and leveled by hand using rakes and garden hoes. A trench of approximately 3.4 m in length was then dug to a depth of about 11 cm by using garden hoes and a sharpshooter. A smooth bed was created at the bottom of the trench for placing the samples by removing the clods and debris. Each treated and untreated cotton fabric sample was placed in a nondecomposing breathable bag (11 × 15 cm) having 1 mm × 2 mm mesh openings. The bags and thus the fabric samples were then placed at the bottom of the trench horizontally, and the trench was filled back with loose soil burying the sample. The tulle resistance to degradation helped to facilitate fabric collection during excavation from the soil. The sample was in contact with the soil through the mesh openings. The study consisted of two treatments (treated and untreated), five excavation times (2, 4, 7, 12, and 16 weeks after burial), and four replicates. The fabrics were excavated at their respective excavation times, air-dried at room temperature, and lightly brushed to remove large soil particles.

2.4. Biodegradation Kinetics. The biodegradation rate of untreated cotton fabric was described by the first-order kinetics model:

$$w_t = w_0 e^{-kt} \quad (1)$$

where w_t is the weight of fabric remaining at a given time, w_0 is the initial weight of the fabric, t is the time in weeks, and k is the first-order rate coefficient. The natural logarithm was applied to both sides of eq 1, resulting in a linear relationship when $\ln(w_t)$ was plotted against t. The value of k was determined from the slope of this linear relationship. The half-life time ($t_{1/2}$), representing the amount of time required for 50% of the fabric to biodegrade, was calculated by using the following equation:

$$t_{1/2} = \frac{\ln 2}{k} \quad (2)$$

2.5. Characterization. Photographs of the samples were taken using a digital camera (RX100, Sony, Tokyo, Japan). Optical microscopic and 3D optical profile images of the samples were obtained in reflection and transmission modes using a digital microscope (KH-8700, Hirox, Tokyo, Japan). Scanning electron microscopy (SEM) images were obtained using a Phenom G6 ProX SEM (Nanoscience Instruments, Phoenix, AZ, USA) with an accelerating voltage of 10 kV. To prepare the sample, it was mounted on a stub using double-sided carbon tape, followed by sputtering a 5 nm-thick gold coating onto the sample. Transmission electron microscopy (TEM) images were obtained using a JEM-2011 TEM (Jeol, Tokyo, Japan) operating at 200 kV. Sample preparation for TEM involved grinding the cotton fabric in a Wiley Mill (Arthur H. Thomas, Philadelphia, PA, USA) through a 60 mesh (250 μm) sieve. The ground sample was placed in a BEEM capsule, and a mixture of methyl methacrylate, butyl methacrylate, and benzoyl peroxide was added to the capsule. The mixture was then polymerized under UV light (CL-1000, UVP, Upland, CA, USA) for 30 min, following published techniques.[27,28] The A block of the embedded sample was cut into approximately 100 nm-thick slices using a PowerTome Ultramicrotome (Boeckeler Instruments, Tucson, AZ, USA). These thin films were placed on a carbon-film-coated copper grid. The photoinitiator (benzoyl peroxide) absorbed UV radiation at a wavelength of 302 nm and initiated the polymerization at room temperature. The size of silver nanoparticles was determined by analyzing TEM micrographs using ImageJ software.[29]

Ultraviolet−visible (UV−vis) spectra were collected by using an ISR-2600 spectrometer (Shimadzu, Kyoto, Japan) equipped with an integrating sphere unit. Absorbance spectra were collected in the wavelength range 200−1100 nm.

Elemental analysis was conducted by using an inductively coupled plasma optical emission spectrometer (ARCOS, Spectro Analytical, Kleve, Germany). Approximately 0.5 g of a ground sample was digested using a digester (HotBlock SC154, Environmental Express, Charleston, SC, USA) in 10.0 mL of concentrated trace metal-grade HNO_3. The total carbon and nitrogen contents of each sample were determined by using a combustion carbon/nitrogen determinator (CN828, LECO, St. Joseph, MI, USA).

2.6. Antifungal Test. *Aspergillus flavus*-70 strain expressing the green fluorescent protein (GFP) (SRRC 1436) was grown in the light at 30 °C on maltose extract agar (Becton Dickinson and Company, Sparks, MD) media following published techniques.[30] Spores of *Aspergillus flavus* 70-GFP were collected using a 0.01% Triton X-100 solution. The spore concentration obtained was approximately 4 × 1 x 10^6 spores/

https://doi.org/10.1021/acsomega.3c09390
ACS Omega 2024, 9, 13017−13027

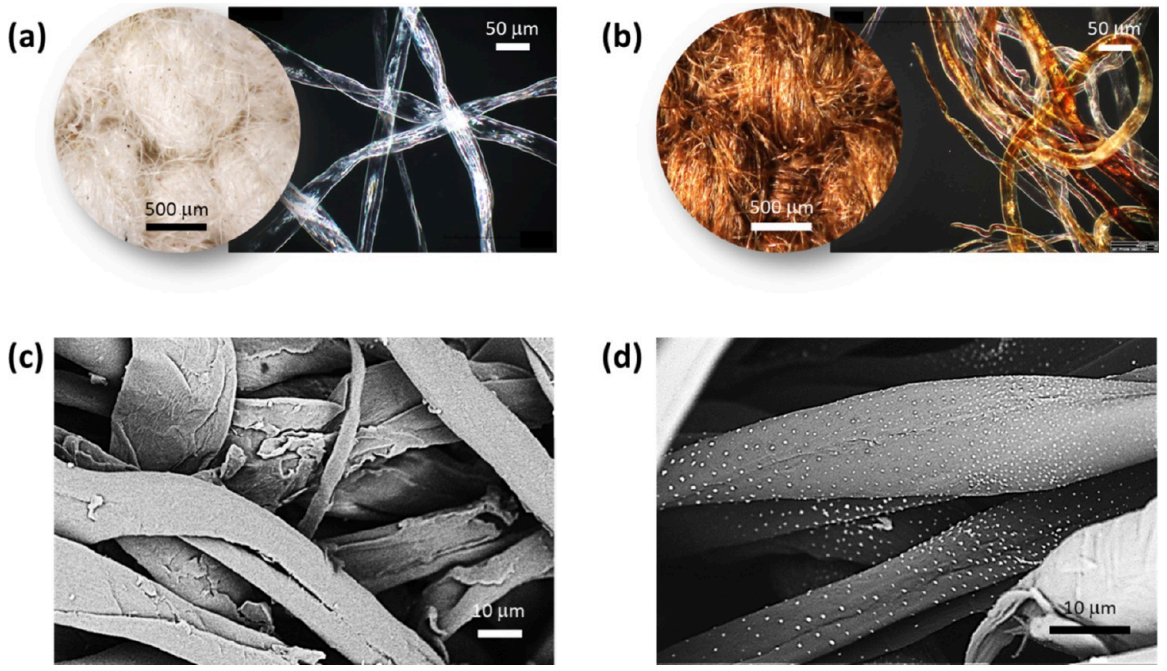

Figure 1. Optical microscopic images of cotton fabrics in reflection mode (left) and cotton fibers in transmission mode (right) (a) before and (b) after the treatment. SEM images of cotton fabrics (c) before and (d) after the treatment.

mL. The spore suspensions were then diluted to a concentration of 4×10^3 spores/mL using a 0.01% Triton X-100 solution. To conduct the antifungal test, 20 mL of the dilute spore suspension was poured into a sterile Petri dish. An autoclaved cotton fabric sample was immersed in the diluted suspension for about 30 s until the fabric became completely saturated. Subsequently, the cotton sample was placed on the surface of a Czapek-Dox agar (BD) plate and gently pressed to ensure contact with the agar surface. The agar plate was then incubated at 30 °C for 3 days. Following the incubation period, photographs of the plates were captured in both bright field and fluorescence modes using an SMZ25 stereo microscope (Nikon Instruments, Melville, NY, USA) equipped with a Zyla 4.2 sCMOS camera (Andor Technology, Belfast, United Kingdom). A quantitative assessment of fungal colonization was conducted by measuring the GFP fluorescence emanating from the fungus. The fabric was cut into circular discs with 7 mm diameter and vortexed in 1 mL of Sorenson's phosphate buffer (pH = 7.0) for 30 s and then centrifuged. The fluorescence of the supernatant was measured at an excitation wavelength of 485 nm and an emission wavelength of 535 nm using a BioTek Synergy Neo2 Hybrid Multimode Reader (Agilent, Santa Clara, CA, USA). The fluorescence of the buffer was also measured as a control.

3. RESULTS AND DISCUSSION

Figure 1 shows optical (top) and SEM (bottom) images of cotton fabrics before and after the treatment. This treatment involved heating a cotton sample in an aqueous solution of $AgNO_3$ at 100 °C. Within 5 min of treatment, the cotton fabric underwent a noticeable transformation, turning brown. This distinct change in color is evident upon comparison of the optical microscopic images of cotton fabrics (Figure 1a,b, left). This coloration was attributed to the formation of silver nanoparticles. Silver nanoparticles possess unique optical properties arising from their surface plasmon resonance. This resonance occurs when the conduction electrons on the surface of nanoparticles oscillate in sync with the electromagnetic light wave of incident light. Depending on the concentration of silver nanoparticles formed within cotton fibers, they impart a spectrum of colors to cotton textiles, ranging from yellow to dark brown.[18,26] Even individual fibers collected from the treated cotton fabric exhibited a vibrant brown hue under transmission mode (Figure 1b, right), indicating a high concentration of silver nanoparticles. The SEM image of the treated cotton fabric shows the formation of numerous nanoparticles on the surface of the cotton fibers (Figure 1d).

In our previous studies,[25,26] we demonstrated that raw cotton fibers possess a remarkable capability to generate silver nanoparticles without the need for external chemical agents, including reducing or stabilizing agents. This unique functionality was attributed to the presence of noncellulosic constituents within raw cotton fibers, specifically pectin, fatty alcohols, sugars, hemicellulose, and proteins. These noncellulosic constituents are plentiful in electron-rich functional groups, enabling them to establish electrostatic interactions with silver cations and convert silver ions into silver atoms.[7,22,25,26] For instance, the oxidation of hydroxyl groups in pectin results in the reduction of silver ions through a series of reactions involving duplicative acetaldehyde oxidation following cyclo-oxo tautomerization.[25] Similarly, galactose-containing vicinal diols in hemicellulose undergo oxidation to form a dialdehyde product, leading to the autoreduction of silver ions. As these noncellulosic constituents are predominantly concentrated in the primary cell wall of cotton fibers (which has a thickness of less than 0.5 μm[31]), most of the nanoparticles were observed to form within the primary cell wall of the cotton fiber.[25,26]

In this study, starch sizing also played a crucial role as a reducing agent. Sizing, a preparatory weaving process, involves applying a natural or synthetic polymer coating to the surface of yarns to enhance their weavability. Starch consists of two primary components—amylose and amylopectin—both con-

https://doi.org/10.1021/acsomega.3c09390
ACS Omega 2024, 9, 13017−13027

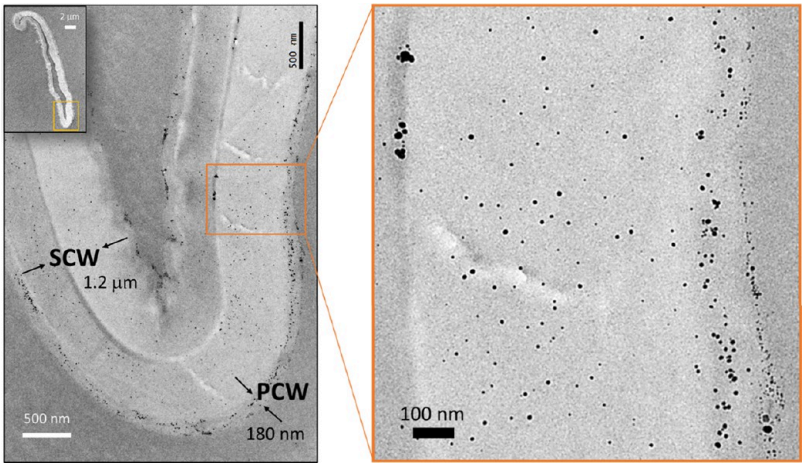

Figure 2. TEM images of cross sections of fibers collected from the treated cotton fabric at various magnifications, showing the formation of silver nanoparticles within both the interior and exterior of the cotton fibers. Rectangular boxes in the left panel images indicate areas of closer examination. Arrows within the image delineate the primary cell wall (PCW) and the secondary cell wall (SCW). Small, black dots in both panels are silver nanoparticles.

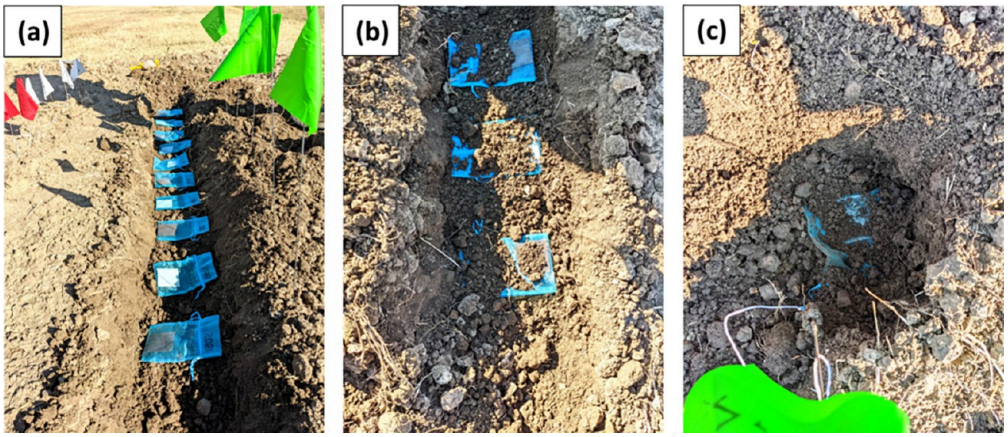

Figure 3. Photographs depicting key stages of the soil burial study: (a) untreated and treated cotton fabrics enclosed in mesh bags before burial, (b) samples were buried in Leeper silty clay loam soil at a depth of 11 cm, and (c) samples excavated after 2, 4, 7, 12, and 16 weeks.

structed from D-glucose molecules. Amylose is a linear polymer characterized by α-1,4- glycosidic linkages, while amylopectin is a branched polymer featuring α-1,6-glycosidic bonds at branching points. When starch is subjected to heating in an aqueous environment, both amylose and amylopectin undergo hydrolysis, generating primary hydroxyl groups capable of reducing silver ions into silver atoms.[32] Furthermore, the oxygen-rich carboxyl and hydroxyl groups of hydrolyzed starch serve to passivate the surface of silver nanoparticles.[32] As a result, silver nanoparticles are evenly dispersed on the fiber surface without any signs of aggregation (Figure 1d).

Figure 2 shows TEM images of cross sections of fibers collected from the treated cotton fabric at varying magnifications. These images reveal the presence of silver nanoparticles not only within the primary cell wall but also within the secondary cell walls of the fibers. It is worth noting that the secondary cell wall is predominantly composed of cellulose, which does not contribute to effective reduction reactions. This is because given the high degree of polymerization of cellulose in typical matured cotton fibers, approximately 20,000 glucose units,[33] the number of available reducing chain ends is negligible. One possible explanation for this complete incorporation of nanoparticles is that those formed by the starch sizing on the fiber surface diffused into the secondary cell wall. In an aqueous solution, cotton fibers undergo significant swelling, increasing their cross-sectional area by approximately 30%.[34] This swelling action opens up the cotton structure, creating internal channels of sufficient size for the nanoparticles to traverse. Due to the high concentration of reducing noncellulosic constituents, a larger amount of nanoparticles were formed within the primary cell wall.

Figure 3 shows photographs captured during the burial study, which took place in a Leeper silty clay loam soil. To facilitate sample retrieval, cotton samples were enclosed in nondecomposing mesh bags, which allowed contact with the soil. These prepared samples were then buried at a depth of 11 cm. At intervals of 2, 4, 7, 12, and 16 weeks of burial, the samples were excavated and subjected to analysis. Figure 4 shows the plots of environmental conditions throughout the soil burial study period spanning October 20, 2022 to February 9, 2023. This data includes daily maximum and minimum soil temperatures measured at a depth of 10 cm, daily maximum and minimum air temperatures, daily maximum and minimum relative humidity levels, and the cumulative total rainfall for each day. The average maximum and minimum soil temperatures were 16.9 and 12.3 °C, respectively.

https://doi.org/10.1021/acsomega.3c09390
ACS Omega 2024, 9, 13017−13027

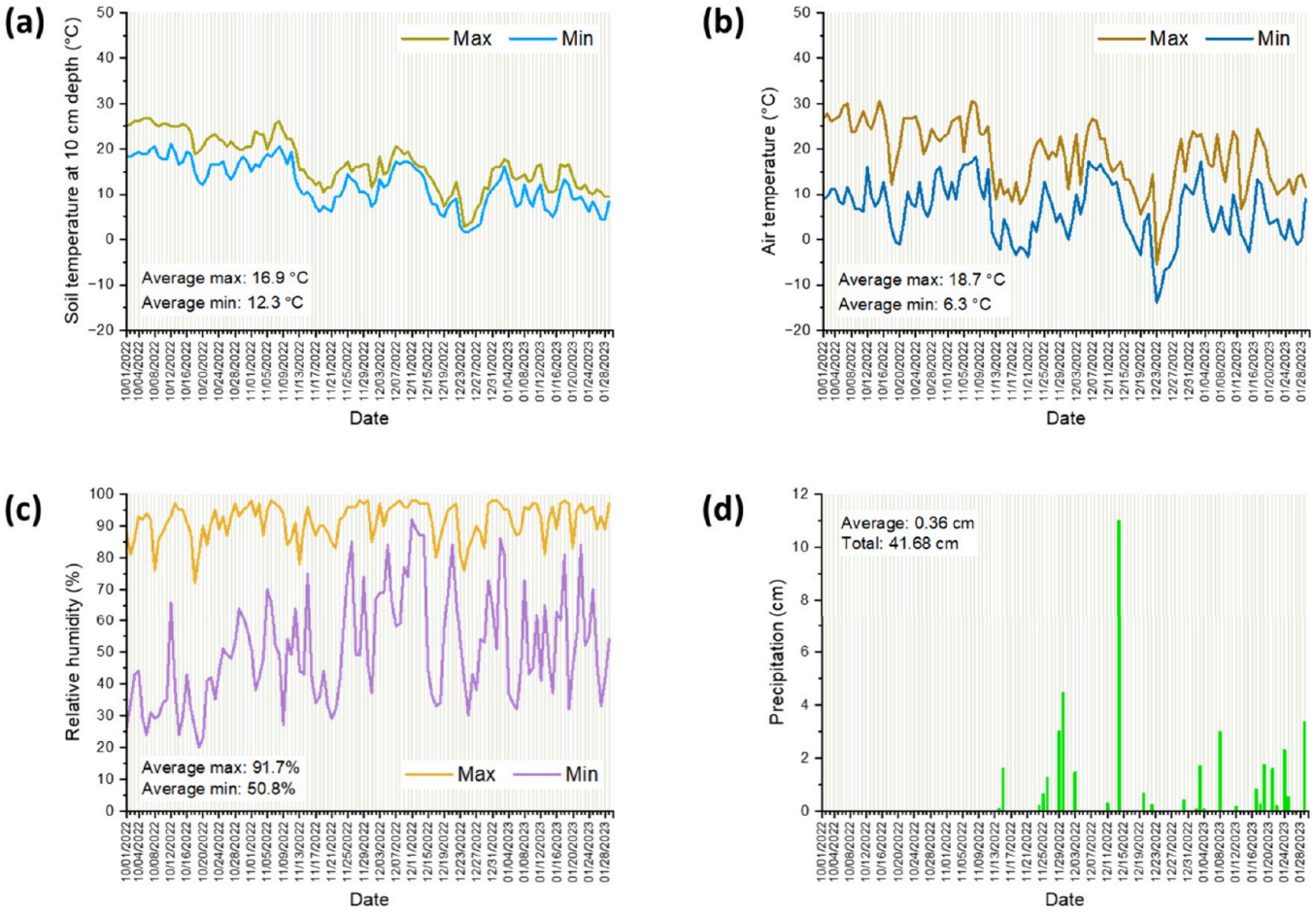

Figure 4. (a) Daily maximum and minimum soil temperatures measured at a depth of 10 cm, (b) daily maximum and minimum air temperatures, (c) daily maximum and minimum relative humidities, and (d) the total rainfall recorded for each day.

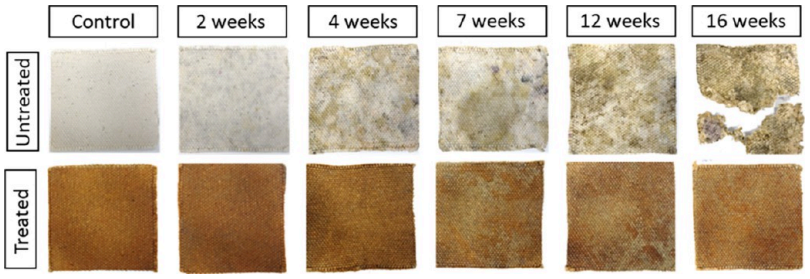

Figure 5. Photographs of untreated and treated cotton fabrics before soil burial and subsequent excavation at 2, 4, 7, 12, and 16 weeks.

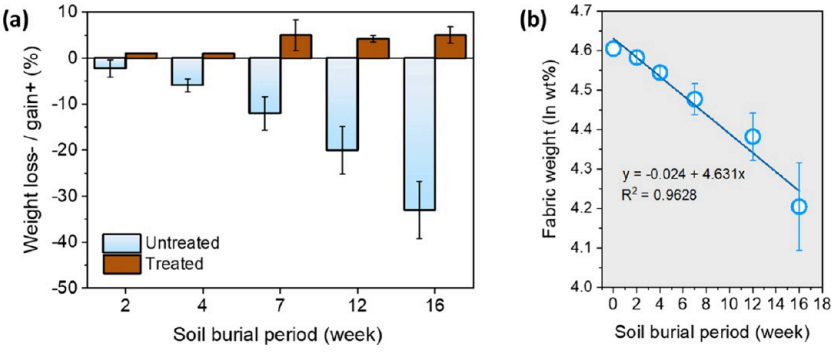

Figure 6. (a) Weight changes observed in untreated and treated cotton fabrics across varying soil burial periods. (b) Seminatural logarithmic plot of fabric weight for untreated cotton fabric vs soil burial period. The solid line represents a fit to the first-order rate equation (eq 1).

https://doi.org/10.1021/acsomega.3c09390
ACS Omega 2024, 9, 13017−13027

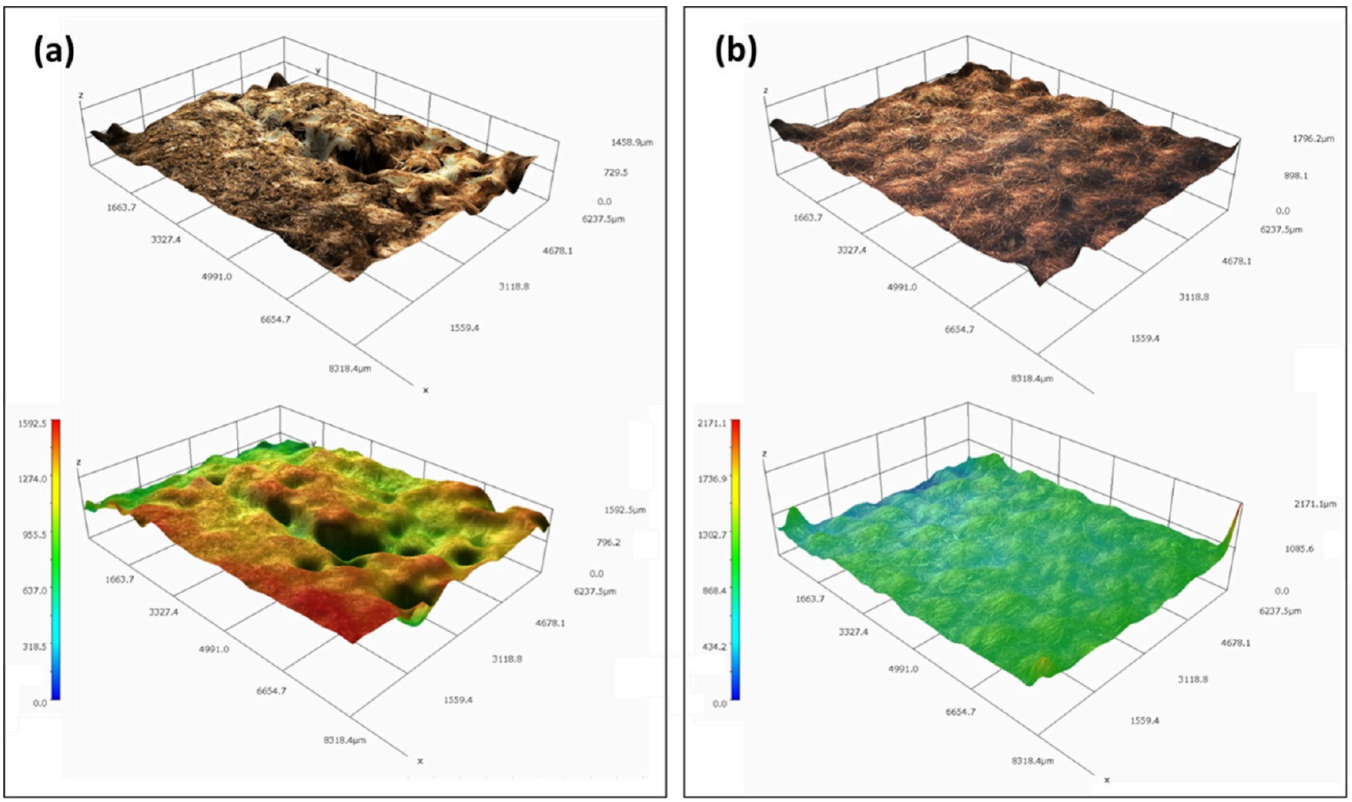

Figure 7. 3D optical profile images of (a) untreated and (b) treated cotton fabrics after 16 weeks of soil burial presented without (top) and with (bottom) color maps.

Figure 5 presents a series of photographs of untreated and treated cotton samples, which were excavated after 2, 4, 7, 12, or 16 weeks of burial, along with their respective samples before burial. This visual representation effectively shows the contrast in degradation between untreated and treated cotton fabrics. At 2 weeks, the untreated fabric exhibited numerous small stains with a blueish hue, indicative of fungal growth. As the burial duration increased, the untreated fabric underwent complete discoloration, featuring patches of brown and black by the later weeks. By the 16 week point, the fabric greatly deteriorated and disintegrated. In contrast, the treated cotton fabric showed no visible signs of degradation throughout the entire 16 week duration. However, an observable amount of soil debris accumulated on the surface of the treated fabric as the soil burial period extended beyond 7 weeks.

The difference in biodegradability between the untreated and treated cotton fabrics is evident in their weight changes, as shown in Figure 6a. The untreated fabric experienced a continuous decline in weight as the soil burial period extended, while the weight of the treated fabric showed a slight increase over longer soil burial periods. These weight gains in the treated fabric were attributed to soil particle adhesion to the fabric surface. The degradation process of cotton cellulose in soil, involving various microorganisms, is complex. Cellulolytic bacteria and fungi in the soil secrete carbohydrate-active enzymes to hydrolyze the β-1,4-glycosidic linkages react with the chain ends of cellulose, or lead to the cleavage of glycosidic bonds.[35] As a result, weight loss was used to measure the rate of biodegradation rather than employing an elementary-reaction-driven approach for the biokinetics.[36] The biodegradation rate of the untreated cotton fabric over the soil burial period was found to follow first-order kinetics, as shown in Figure 6b. Based on eqs 1 and 2, the first-order rate coefficient (k) and the half-life value ($t_{1/2}$) for the untreated cotton fabric were determined to be 0.024 and 28.9 weeks, respectively. It is important to note that the kinetics of cotton textile degradation are influenced by factors such as fabric structure, fabric weight, soil temperatures, and soil moisture.[37] Upon excavation at 16 weeks, the untreated fabric exhibited a substantial weight loss of more than 30%. This loss corresponded with a dramatic change in its 3D profile, revealing a severe disruption in the fabric's structural integrity (Figure 7a). Notably, the untreated cotton fabric featured extensive damage, including the formation of large holes. In contrast, the treated cotton fabric maintained its woven structure without any significant alterations to the surface morphology.

Figure 8 shows SEM images of untreated cotton fabrics excavated at 2, 4, 7, 12, and 16 weeks of soil burial, captured at both low (left) and high (right) magnifications. These images reveal an interesting sequence of degradation stages in cotton fibers—fibrillation, fractionation, and merging—during the soil burial study. At 2 weeks, cotton fibers retained their characteristic flat and twisted ribbon-like morphology, exhibiting no significant morphological alterations or damages. However, by 4 weeks, fibrillation of cotton fibers became evident. Corresponding SEM images show individual fibrils or microfibers disintegrating or fraying from cotton fibers. This fibrillation intensified as the soil burial period was extended to 7 weeks. By 12 weeks, cotton fibers began to break into pieces, ultimately leading to the complete disruption of fiber morphology. As the soil burial reached 16 weeks, the disintegrated cotton fibers merged with each other. Figure 9 shows SEM images for treated cotton fabrics. In contrast to the

https://doi.org/10.1021/acsomega.3c09390
ACS Omega 2024, 9, 13017−13027

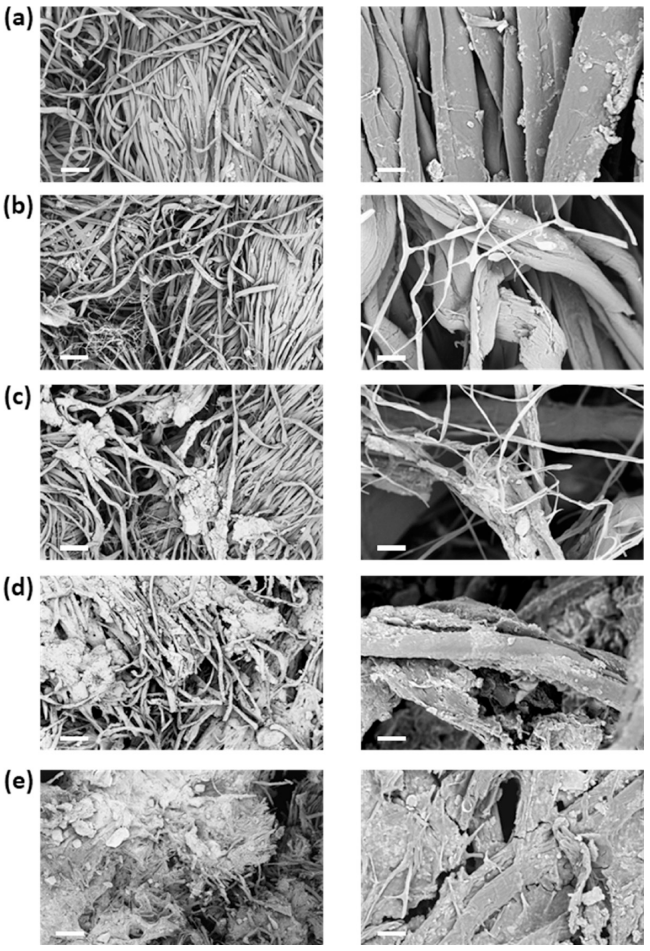

Figure 8. SEM images of untreated cotton fabrics excavated at (a) 2, (b) 4, (c) 7, (d) 12, and (e) 16 weeks during soil burial, which were taken at 500× (left) and 5000× (right) magnifications with scale bars of 100 and 10 μm, respectively.

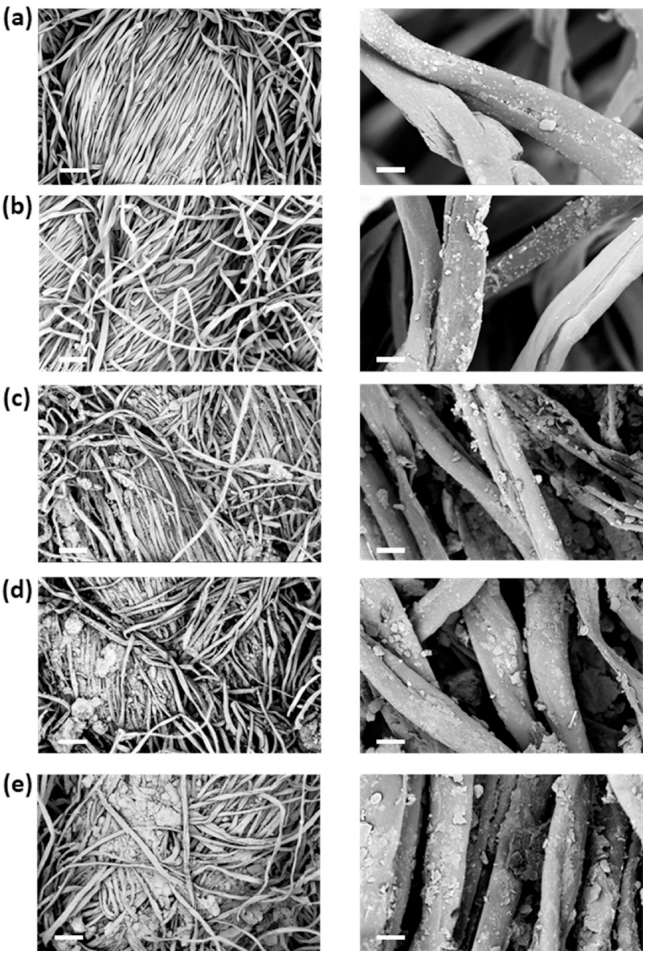

Figure 9. SEM images of treated cotton fabrics excavated at (a) 2, (b) 4, (c) 7, (d) 12, and (e) 16 weeks during soil burial, which were taken at 500× (left) and 5000× (right) magnifications with scale bars of 100 and 10 μm, respectively.

untreated samples, structural deterioration, such as breakages or cracks, was rarely observed in the treated cotton fibers throughout the entire duration of the soil burial study. Consistent with the findings of weight changes (Figure 6a), at 7 weeks, a relatively substantial amount of soil particles began adhering to the surface of the cotton fibers.

Next, we investigated the impact of soil burial on the silver nanoparticles incorporated into cotton fibers. Figure 10a shows the UV−vis spectra of treated cotton fabrics across different excavation periods. The treated fabric, prior to soil burial, exhibited a surface plasmon resonance peak centered at around 425 nm, confirming the presence of silver nanoparticles.[25] This surface plasmon resonance peak exhibited minimal variation for 4 weeks. However, at 7 weeks, significant alterations in both the intensity and shape of the peak became apparent—specifically, a blue shift to 370 nm with reduced intensity. This shift coincided with the 7 week soil burial period when soil particles started adhering to the fabric surface (Figures 5 and 6a). Upon contact with soil, silver nanoparticles have the potential to interact with soil minerals, undergoing oxidative transformations, followed by reactions with dissolved silver ions to generate AgCl and Ag_2S phases[38,39] or forming complexes with soil components, such as metal oxides[40] and organic matter.[41] The depletion pattern of silver during soil burial was monitored by measuring the silver concentration in the cotton fabric. As can be seen in Figure 10b, the silver concentration gradually declined up to 7 weeks, after which it remained relatively constant during longer burial periods. It is plausible to consider that silver nanoparticles formed on the surface of cotton fibers are involved in silver loss because they are susceptible to adsorption or binding with clay particles and organic substances. In contrast, the silver nanoparticles located within the interior of the cotton fibers were shielded from interactions with soil. This resistance to migration of interior nanoparticles was confirmed by the TEM image of the cross-section of treated cotton fibers excavated after 16 weeks (Figure 10c). Many nanoparticles remained evenly dispersed within the cotton fibers, exhibiting no signs of aggregation, similar to their states before burial.

We analyzed the variations in macroelements and trace elements within the treated cotton fabrics as the soil burial period was extended (Figure 11). Carbon (C) was the predominant element in cotton fabric, and its concentration showed a slight decrease with increasing soil burial duration. Additionally, cotton fabric contained trace amounts of nitrogen (N) and various inorganic elements, such as calcium (Ca), phosphorus (P), potassium (K), sulfur (S), magnesium (Mg), and sodium (Na). Among the macroelements, Ca was relatively more abundant. The concentrations of N, Ca, K, and Mg exhibited slight increases with longer soil burial

https://doi.org/10.1021/acsomega.3c09390
ACS Omega 2024, 9, 13017−13027

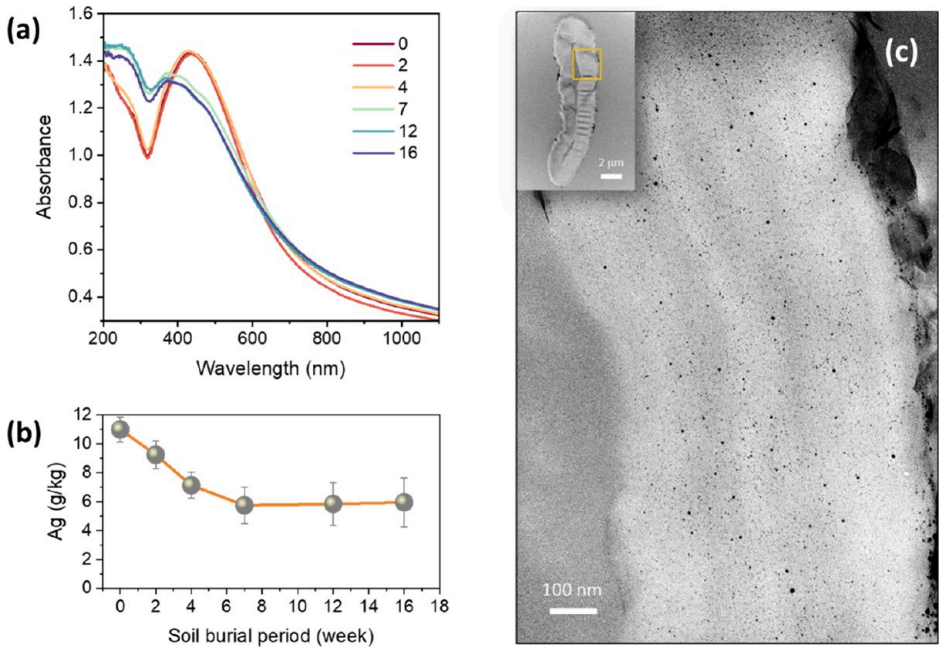

Figure 10. (a) UV−vis spectra of treated cotton fabrics excavated after 2, 4, 7, 12, and 16 weeks of soil burial. (b) Silver concentration in treated cotton fabric as a function of the soil burial period. (c) TEM image of the cross-section of cotton fiber from the treated cotton fabric excavated after 16 weeks of soil burial. The inset shows a low-magnification TEM image with a rectangular box indicating the region of the higher-magnification image taken.

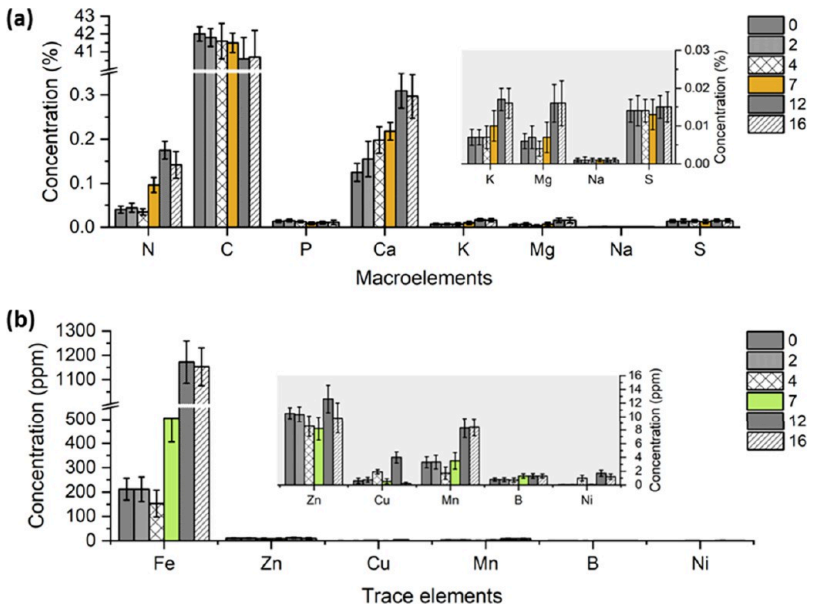

Figure 11. Concentrations of (a) macroelements and (b) trace elements in the treated cotton fabrics excavated after 2, 4, 7, 12, and 16 weeks of soil burial. The insets show plots for low-concentration elements with adjusted *y*-axis scales.

periods. In terms of trace elements, iron (Fe) dominated, and its concentration began to rise after 7 weeks. These changes in the concentrations of macroelements and trace elements were attributed to the adsorption of soil onto the fabric.

The antifungal properties of silver nanoparticles were considered to be one of the major contributing factors to the remarkable resistance of the treated cotton fabric against biodegradation in soil. Figure 12 shows the results of testing using the saprophytic soil-borne fungus *Aspergillus flavus* (*A. flavus*). This fungus is known to produce carcinogenic aflatoxins in lipid-rich seeds, such as cotton, corn, peanuts, and tree nuts, during plant growth. To effectively analyze fungal growth on cotton fabric, *A. flavus* was engineered to express GFP derived from the jellyfish *Aequorea victoria*. This modified strain served as a visual indicator for evaluating *A. flavus* colonization on cotton fabric, offering both qualitative and quantitative results. As presented in the photographs of the inoculated cotton fabrics (Figure 12a), fungal proliferation and colonization were conspicuous on the untreated cotton fabric, whereas no observable fungal growth occurred on the treated cotton fabric. Under white light microscopy, the woven structure of the untreated cotton fabric was obscured by

https://doi.org/10.1021/acsomega.3c09390
ACS Omega 2024, 9, 13017−13027

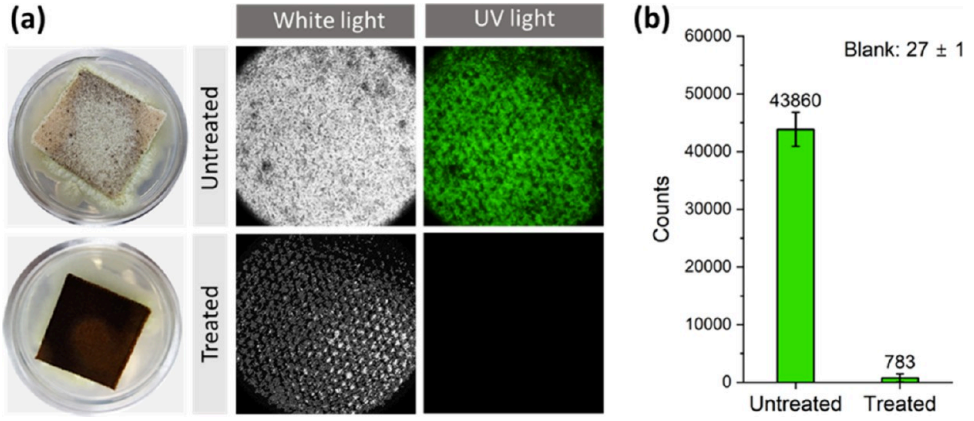

Figure 12. (a) Photographs and microscopic images under white and UV light for untreated and treated cotton fabrics inoculated with GFP-expressing *A. flavus* 70. (b) GFP fluorescence for untreated and treated cotton fabrics.

fungal growth. Under UV light, the GFP green fluorescence emitted by the fungus was prominent on the untreated fabric. Conversely, minimal fluorescence was detected on the treated cotton fabric. The extent of fungal colonization, quantified by measuring GFP fluorescence on the treated cotton fabric, was found to be 56-fold lower than that on the untreated cotton fabric (Figure 12b). These results validate the powerful antifungal properties of silver nanoparticles.

CONCLUSIONS

Silver nanoparticles represent highly sought-after agents in the textile industry for the production of odor-inhibiting and anti-infective textiles. Various nanoparticle finishing methods, ranging from surface coatings to intercalation, have been developed. However, there is limited knowledge of the biodegradation behaviors of cotton fibers doped with silver nanoparticles on the fiber surface and throughout the fiber cross section. In this study, we introduced both interior (18 ± 4 nm) and exterior (126 ± 17 nm) silver nanoparticles to cotton fibers with a total concentration of 11 g/kg and conducted a soil burial study. This *in situ* synthesis was achieved by using the noncellulosic constituents present in raw cotton fibers and starch sizing as reducing agents, obviating the necessity for additional agents. Notably, the treated cotton fabric exhibited strong resistance to biodegradation in soil, maintaining fabric and fiber structural integrity even after 16 weeks of burial, a period during which the untreated fabric disintegrated, losing more than 30% of its weight. The diminished biodegradability observed in the treated cotton fabric was ascribed to the potent antimicrobial properties of the silver nanoparticles. When tested with the GFP-expressing soil-borne fungus *A. flavus*, the treated cotton fabric emitted minimal green fluorescence and exhibited a 56-fold reduction in fungal growth compared to the untreated cotton fabric. As for the behavior of silver, there was an initial increase in its rate of loss over time followed by a plateau. This nonlinear pattern suggests that the depletion of nanoparticles from the cotton fabric is influenced by their location, whether they are present in the interior or exterior of the cotton fiber.

AUTHOR INFORMATION

Corresponding Author

Sunghyun Nam − *U.S. Department of Agriculture, Agricultural Research Service, Southern Regional Research Center, New Orleans, Louisiana 70124, United States;* orcid.org/0000-0002-4059-606X; Phone: +1 504 286 4229; Email: sunghyun.nam@usda.gov; Fax: +1 504 286 4390

Authors

Haile Tewolde − *U.S. Department of Agriculture, Agricultural Research Service, Crop Science Research Laboratory, Mississippi State, Mississippi 39762, United States*

Zhongqi He − *U.S. Department of Agriculture, Agricultural Research Service, Southern Regional Research Center, New Orleans, Louisiana 70124, United States*

Kanniah Rajasekaran − *U.S. Department of Agriculture, Agricultural Research Service, Southern Regional Research Center, New Orleans, Louisiana 70124, United States*

Jeffrey W. Cary − *U.S. Department of Agriculture, Agricultural Research Service, Southern Regional Research Center, New Orleans, Louisiana 70124, United States*

Gregory Thyssen − *U.S. Department of Agriculture, Agricultural Research Service, Southern Regional Research Center, New Orleans, Louisiana 70124, United States*

Hailin Zhang − *Department of Plant and Soil Sciences, Oklahoma State University, Stillwater, Oklahoma 74078, United States*

Christine Sickler − *U.S. Department of Agriculture, Agricultural Research Service, Southern Regional Research Center, New Orleans, Louisiana 70124, United States*

Md Muhaiminul Islam − *U.S. Department of Agriculture, Agricultural Research Service, Southern Regional Research Center, New Orleans, Louisiana 70124, United States; Department of Chemistry, Tulane University, New Orleans, Louisiana 70118, United States;* orcid.org/0009-0007-0285-8632

Complete contact information is available at: https://pubs.acs.org/10.1021/acsomega.3c09390

Notes

The authors declare no competing financial interest.

ACKNOWLEDGMENTS

This research was supported by the ARS Innovation Fund. The authors would like to thank Dr. Dongmei Cao at the LSU Shared Instrument Facility for their assistance in data collection. This research was supported by the U.S. Department of Agriculture, Agricultural Research Service. Mention of trade names or commercial products is solely for the purpose

https://doi.org/10.1021/acsomega.3c09390
ACS Omega 2024, 9, 13017−13027

of providing specific information and does not imply recommendation or endorsement by USDA. USDA is an equal opportunity provider and employer.

REFERENCES

(1) Khan, S.; Mansoor, S.; Rafi, Z.; Kumari, B.; Shoaib, A.; Saeed, M.; Alshehri, S.; Ghoneim, M. M.; Rahamathulla, M.; Hani, U.; et al. A review on nanotechnology: Properties, applications, and mechanistic insights of cellular uptake mechanisms. *J. Mol. Liq.* **2022**, *348*, No. 118008.

(2) Grasso, G.; Zane, D.; Dragone, R. Microbial nanotechnology: Challenges and prospects for green biocatalytic synthesis of nanoscale materials for sensoristic and biomedical applications. *Nanomaterials* **2020**, *10* (1), 11.

(3) Guerra, F. D.; Attia, M. F.; Whitehead, D. C.; Alexis, F. Nanotechnology for environmental remediation: Materials and applications. *Molecules* **2018**, *23*, 1760.

(4) Shastri, J. P.; Rupani, M. G.; Jain, R. L. Antimicrobial activity of nanosilver-coated socks fabrics against foot pathogens. *J. Text. Inst.* **2012**, *103*, 1234−1243.

(5) Lok, C. N.; Ho, C. M.; Chen, R.; He, Q. Y.; Yu, W. Y.; Sun, H.; Tam, P. K.; Chiu, J. F.; Che, C. M. Silver nanoparticles: partial oxidation and antibacterial activities. *J. Biol. Inorg. Chem.* **2007**, *12* (4), 527−534.

(6) Nam, S.; Park, B.; Condon, B. D. Water-based binary polyol process for the controllable synthesis of silver nanoparticles inhibiting human and foodborne pathogenic bacteria. *RSC Adv.* **2018**, *8*, 21937−21947.

(7) Nam, S.; Baek, I. S.; Hillyer, M. B.; He, Z.; Barnaby, J. Y.; Condon, B. D.; Kim, M. S. Thermosensitive textiles made from silver nanoparticle-filled brown cotton fibers. *Nanoscale Adv.* **2022**, *4*, 3725−3736.

(8) Park, M.; Im, J.; Shin, M.; Min, Y.; Park, J.; Cho, H.; Park, S.; Shim, M. B.; Jeon, S.; Chung, D. Y.; et al. Highly stretchable electric circuits from a composite material of silver nanoparticles and elastomeric fibres. *Nat. Nanotechnol.* **2012**, *7* (12), 803−809.

(9) Montazer, M.; Allahyarzadeh, V. Electroless plating of silver nanoparticles/nanolayer on polyester fabrci using $AgNO_3$/NaOH and ammonia. *Ind. Eng. Chem. Res.* **2013**, *52* (25), 8436−8444.

(10) Tang, B.; Zhang, M.; Hou, X.; Li, J.; Sun, L.; Wang, X. Coloration of cotton fibers with anisotropic silver nanoparticles. *Ind. Eng. Chem. Res.* **2012**, *51*, 12807−12813.

(11) Kelly, F. M.; Johnston, J. H. Colored and functional silver nanoparticle-wool fiber composites. *ACS Appl. Mater. Interfaces* **2011**, *3*, 1083−1092.

(12) Lee, H. J.; Yeo, S. Y.; Jeong, S. H. Antibacterial effect of nanosized silver colloidal solution on textile fabrics. *J. Mater. Sci.* **2003**, *38*, 2199−2204.

(13) He, J.; Kunitake, T.; Nakao, A. Facile in situ synthesis of noble metal nanoparticles in porous cellulose fibers. *Chem. Mater.* **2003**, *15*, 4401−4406.

(14) Lee, H. Y.; Park, H. K.; Lee, Y. M.; Kim, K.; Park, S. B. A practical procedure for producing silver nanocoated fabric and its antibacterial evaluation for biomedical applications. *Chem. Commun.* **2007**, *28*, 2959−2961.

(15) Vigneshwaran, N.; Kathe, A. A.; Varadarajan, P. V.; Nachane, R. P.; Balasubramanya, R. H. Functional finishing of cotton fabrics using silver nanoparticles. *J. Nanosci. Nanotechnol.* **2007**, *7* (6), 1893−1897.

(16) Lorenz, C.; Windler, L.; von Goetz, N.; Lehmann, R. P.; Schuppler, M.; Hungerbühler, K.; Heuberger, M.; Nowack, B. Characterization of silver release from commercially available functional (nano)textiles. *Chemosphere* **2012**, *89*, 817−824.

(17) Geranio, L.; Heuberger, M.; Nowack, B. The behavior of silver nano textiles during washing. *Environ. Sci. Technol.* **2009**, *43*, 8113−8118.

(18) Nam, S.; Condon, B. Internally dispersed synthesis of uniform silver nanoparticles via in situ reduction of $[Ag(NH_3)_2]^+$ along natural microfibrillar substructures of cotton fiber. *Cellulose* **2014**, *21*, 2963−2972.

(19) Nam, S.; Condon, B. D.; Delhom, C. D.; Fontenot, K. R. Silver-cotton nanocomposites: Nano-design of microfibrillar structure causes morphological changes and increased tenacity. *Sci. Rep.* **2016**, *6*, 37320.

(20) Nam, S.; Hillyer, M. B.; Condon, B. D.; Lum, J. S.; Richards, M. N.; Zhang, Q. Nanoparticle-infused cotton fiber: Durability and aqueous release of silver in laundry water. *J. Agric. Food Chem.* **2020**, *68*, 13231−13240.

(21) Edwards, J. V.; Prevost, N.; Yager, D.; Nam, S.; Graves, E.; Santiago, M.; Condon, B.; Dacorta, J. Antimicrobial and hemostatic activities of cotton-based dressings designed to address prolonged field care applications. *Mil. Med.* **2021**, *186*, 116−121.

(22) Nam, S.; Selling, G. W.; Hillyer, M. B.; Condon, B. D.; Rahman, M. S.; Chang, S. Brown cotton fibers self-produce Ag nanoparticles for regenerating their antimicrobial surfaces. *ACS Appl. Nano Mater.* **2021**, *12*, 13112−13122.

(23) Hillyer, M. B.; Nam, S.; Condon, B. D. Intrafibrillar dispersion of cuprous oxide (Cu_2O) nanoflowers within cotton cellulosic fabrics for permanent antibacterial, antifungal, and antiviral activity. *Molecules* **2022**, *27*, 7706.

(24) Hillyer, M. B.; Jordan, J. H.; Nam, S.; Easson, M. W.; Condon, B. D. Silver nanoparticle-intercalated cotton fiber for catalytic degradation of aqueous organic dyes for water pollution mitigation. *Nanomaterials* **2022**, *12*, 1621.

(25) Nam, S.; Hillyer, M. B.; He, Z.; Chang, S.; Edwards, J. V. Self-induced transformation of raw cotton to a nanostructured primary cell wall for a renewable antimicrobial surface. *Nanoscale Adv.* **2022**, *4*, 5404−5416.

(26) Nam, S.; Hinchliffe, D. J.; Hillyer, M. B.; Gary, L.; He, Z. Washable Antimicrobial Wipes Fabricated from a Blend of Nano-composite Raw Cotton Fiber. *Molecules* **2023**, *28*, 1051.

(27) Thibodeaux, D. P.; Evans, J. P. Cotton fiber maturity by image analysis. *Text. Res. J.* **1986**, *56*, 130−139.

(28) Boylston, E. K.; Hinojosa, O.; Hebert, J. J. A quick embedding method for light and electron microscopy of textile fibers. *Biotechnol. Histochem.* **1991**, *66* (3), 122−124.

(29) Schneider, C. A.; Rasband, W. S.; Eliceiri, K. W. NIH Image to ImageJ: 25 years of image analysis. *Nat. Methods* **2012**, *9*, 671−675.

(30) Rajasekaran, K.; Cary, J. W.; Cotty, P. J.; Cleveland, T. E. Development of a GFP-expressing *Aspergillus flavus* Strain to study fungal invasion, colonization, and resistance in cottonseed. *Mycopathologia* **2008**, *165*, 89−97.

(31) Maxwell, J. M.; Gordon, S. G.; Huson, M. G. Internal structure of mature and immature cotton fibers revealed by scanning probe microscopy. *Text. Res. J.* **2003**, *73*, 1005−1012.

(32) Ponsanti, K.; Tangnorawich, B.; Ngernyuang, N.; Pechyen, C. A flower shape-green synthesis and characterization of silver nanoparticles (AgNPs with different starch as a reducing agent. *J. Mater. Res. Technol.* **2020**, *9*, 11003−11012.

(33) Wakelyn, P. J.; Bertoniere, N. R.; French, A. D.; Thibodeaux, D. P.; Triplett, B. A.; Rousselle, M.-A.; Goynes, W. R. Jr.; Edwards, J. V.; Hunter, L.; McAlister, D. D.; et al. *Cotton Fiber Chemistry and Technology*; CRC Press, 2006.

(34) Moore, A. T.; Scott, L. W.; deGruy, I. V.; Rollins, M. L. The swelling of cotton in water: A microscopical study. *Text. Res. J.* **1950**, *20*, 620−630.

(35) Wilson, D. B. Three Microbial Strategies for Plant Cell Wall Degradation. *Ann. N.Y. Acad. Sci.* **2008**, *1125*, 289−297.

(36) Loccufier, E.; Deventer, K.; Manhaeghe, D.; Van Hulle, S. W. H.; D'hooge, D. R.; De Buysser, K.; De Clerck, K. Degradation kinetics of isoproturon and its subsequent products in contact with TiO2 functionalized silica nanofibers. *Chem. Eng. J.* **2020**, *387*, No. 124143.

(37) Nam, S.; Slopek, R.; Wolf, D.; Warnock, M.; Condon, B. D.; Sawhney, P.; Gbur, E.; Reynolds, M.; Allen, C. Comparison of biodegradation of low-weight hydroentangled raw cotton nonwoven

https://doi.org/10.1021/acsomega.3c09390
ACS Omega 2024, 9, 13017−13027

fabric and that of commonly used disposable nonwoven fabrics in aerobic Captina silt loam soil. *Text. Res. J.* **2016**, *86*, 155−166.
(38) Cornelis, G.; Pang, L.; Doolette, C.; Kirby, J. K.; McLaughlin, M. J. Transport of silver nanoparticles in saturated columns of natural soils. *Sci. Total Environ.* **2013**, *463*−*464*, 120−130.
(39) Levard, C.; Hotze, E. M.; Lowry, G. V.; Brown, J. G. E. Environmental transformations of silver nanoparticles: impact on stability and toxicity. *Environ. Sci. Technol.* **2012**, *46*, 6900−6914.
(40) Cornelis, G.; Doolette, C.; Thomas, M.; McLaughlin, M. J.; Kirby, J. K.; Beak, D. G.; Chittleborough, D. Retention and dissolution of engineered silver nanoparticles in natural soils. *Soil Sci. Soc. Am. J.* **2012**, *76*, 891−902.
(41) Jones, K. C.; Davies, B. E.; Peterson, P. J. Silver in Welsh soils: Physical and chemical distribution studies. *Geoderma* **1986**, *37*, 157−174.

https://doi.org/10.1021/acsomega.3c09390
ACS Omega 2024, 9, 13017−13027